Published in final edited form as:
Cell Rep. 2013 November 14; 5(3): . doi:10.1016/j.celrep.2013.09.041.

A molecular mechanism regulating the timing of corticogeniculate innervation

Justin M. Brooks[1,3], **Jianmin Su**[1], **Carl Levy**[2], **Jessica S. Wang**[3], **Tania A. Seabrook**[3,4], **William Guido**[3,4], and **Michael A. Fox**[1,2,3,*]

[1]Virginia Tech Carilion Research Institute, Roanoke VA 24016

[2]Department of Biological Sciences, Virginia Tech, Blacksburg, VA 24061

[3]Department of Anatomy and Neurobiology, Virginia Commonwealth University, Richmond, VA 23298

[4]Department of Anatomical Sciences & Neurobiology, University of Louisville, Louisville, KY 40202

SUMMARY

Neural circuit formation demands precise timing of innervation by different classes of axons. However the mechanisms underlying such activity remain largely unknown. In the dorsal lateral geniculate nucleus (dLGN), axons from the retina and visual cortex innervate thalamic relay neurons in a highly coordinated manner, with those from the cortex arriving well after those from retina. The differential timing of retino- and corticogeniculate innervation is not a coincidence but is orchestrated by retinal inputs. Here, we identified a chondroitin sulfate proteoglycan (CSPG) that regulates the timing of corticogeniculate innervation. Aggrecan, a repulsive CSPG, is enriched in neonatal dLGN and inhibits cortical axons from prematurely entering the dLGN. Postnatal loss of aggrecan from dLGN coincides with upregulation of aggrecanase expression in the dLGN and corticogeniculate innervation and, importantly, is regulated by retinal inputs. Taken together, these studies reveal a molecular mechanism through which one class of axons coordinates the temporal targeting of another class of axons.

INTRODUCTION

Neural circuit formation requires precise spatial and temporal targeting of axons to appropriate brain regions. For decades the visual system has served as a model system to explore the cellular and molecular mechanisms that govern these aspects of neural circuit formation. In particular, mechanisms underlying axonal guidance, axonal targeting of distinct nuclei (or regions within these nuclei), and the sorting of axons into topographic maps have been elucidated by studying retinofugal circuits (Huberman et al. 2008; Sanes and Zipursky 2010; Fox and Guido 2011). While most of these studies have focused on the mechanism of spatial targeting of axons, the visual system also offers the opportunity to explore mechanisms underlying the timing of innervation by different classes of axons. In the dLGN, retinal and cortical axons arrive and innervate thalamic relay neurons

Corresponding Author: Michael A. Fox, Ph.D., Virginia Tech Carilion Research Institute, 2 Riverside Circle, Roanoke, VA 24016, Phone: (540) 526-2050, mafoxl@vtc.vt.edu.

asynchronously, with those from the cortex arriving well after those from retina (Shatz and Rakic 1981; Seabrook et al. 2013). Despite the significant delay in corticogeniculate innervation (compared with retinogeniculate projections), cortical axons accumulate at the border of the dLGN and appear to be "waiting" for the proper time to enter and arborize in dLGN (Jacobs et al. 2007; Grant et al. 2012)(Figure 1A). We recently reported that the timing of cortical axon entry into dLGN coincides with the remodeling of retinal axons and appears to be orchestrated by these retinal inputs (Seabrook et al. 2013). This implies a new level of coordination in thalamic circuit development. If cortical axons are indeed "waiting" for the proper time to innervate dLGN, we postulate that an underlying molecular mechanism must exist that is regulated by retinal input. In the present study we sought to uncover such a mechanism. We discovered that aggrecan, a repulsive chondroitin sulfate proteoglycan (CSPG), is enriched in perinatal dLGN and we applied *in vitro* and *in vivo* approaches to illustrate its role in regulating the timing of cortical axon invasion into dLGN. Importantly, we demonstrate that retinal inputs play an instructive role in regulating aggrecan distribution in dLGN.

RESULTS

Developmental regulation of aggrecan in dLGN

Cortical axon growth and entry into dLGN was assessed by immunostaining tissue from *golli-tau-gfp* reporter mice, in which layer VI neurons are selectively labeled with tau-GFP (Figure 1B)(Jacobs et al. 2007). Axons from layer VI cortical neurons appear adjacent to the ventro-medial border of dLGN shortly after birth, but fail to invade dLGN until postnatal day 4 (P4)(Figure 1 A, B and Seabrook et al. 2013). We therefore hypothesized that a repulsive cue must be present in neonatal dLGN to prevent premature CG innervation. To identify such a cue, we initially profiled the transcriptome of P3 and P8 dLGN, with the assumption that mRNA of repulsive cues inhibiting premature CG innervation would be down-regulated as cortical axons begin to enter dLGN. No such molecules were identified (data not shown). As an alternative approach we applied a candidate screen for CSPGs in neonatal dLGN. This family of extracellular matrix (ECM) molecules has well-established roles in inhibiting the growth of axons (Kwok et al. 2008; Zimmerman and Dours-Zimmerman 2008). We focused on the distribution of 5 CSPGs: brevican, neurocan, versican, phosphacan and aggrecan. Little if any brevican, neurocan, versican, and phosphacan were observed in neonatal mouse dLGN (Figure 1C). In contrast, aggrecan was significantly enriched in dLGN and other regions of dorsal thalamus (Figure 1C, D). Although enriched in dLGN at postnatal day 0 (P0), aggrecan was absent from the external medullary lamina (eml) – the pathway by which cortical axons approach the dLGN after traveling through the internal capsule (see arrows in Figure 1C, D). To confirm the specificity of aggrecan-IR we immunostained brain sections from an autosomal recessive mouse mutant lacking aggrecan (*acan*^{cmd})(Watanabe et al. 1994). The lack of aggrecan-IR in *acan*^{cmd} dLGN confirmed the specificity of aggrecan-IR in dLGN (Figure 1D).

Although robustly expressed at birth, we observed a progressive loss of aggrecan-IR from dorsal thalamus during postnatal development (Figure 1D). The loss of aggrecan in dLGN coincided with CG innervation. To definitively test this observation, we assessed aggrecan-IR in *golli-tau-gfp* reporter mice. Not only did the area of dLGN occupied by aggrecan-IR inversely correlate with the area of dLGN occupied by GFP-positive CG axons (Figure 1E, F) but the first regions to lack aggrecan (i.e ventro-medial dLGN) were the first regions innervated by cortical axons (Figure 1E, G, H).

Aggrecan prevents cortical axon growth into dLGN

Based upon the known role of aggrecan in inhibiting axonal growth, these expression analyses suggest that the distribution of aggrecan influences when and where cortical axons invade dLGN. For aggrecan to influence corticogeniculate innervation, we hypothesized that layer VI cortical neurons must express a subset of aggrecan/CSPG receptors, such as Nogo Receptors (NgRs) or Protein Tyrosine Phosphatase Receptors (PTPRs) (Shen et al. 2009; Fisher et al. 2011; Dickendesher et al. 2012). Previous reports have demonstrated NgR-expression in neonatal cortical neurons (Xiaolei et al. 2009; Wang et al. 2008) and we found that aggrecan-binding PTPRs are expressed by layer VI neurons (Figure S1). Thus, cortical neurons have the machinery to respond to aggrecan.

To test whether aggrecan inhibited layer VI cortical axon outgrowth we developed an *in vitro* modified stripe assay in which various concentrations of aggrecan were presented to GFP-expressing cortical axons isolated from *golli-tau-gfp* mice. In these assays GFP-containing neurites grew into regions containing no or low concentrations of aggrecan (Figure 2A, E). In contrast, high concentrations of aggrecan potently repelled layer VI cortical neurites (Figure 2B, C, E). To ensure that these results were not due to a physical boundary, we treated aggrecan with chondroitinase ABC (chABC), a bacterial enzyme that efficiently cleaves the inhibitory glycosaminoglycan (GAG) sidechains from CSPGs. Pretreatment with chABC significantly reduced the ability of aggrecan to inhibit neurite outgrowth of layer VI cortical neurons (Figure 2D, E).

Since our *in vitro* data demonstrates aggrecan is sufficient to inhibit the outgrowth of cortical axons, we next explored whether removal of aggrecan accelerated CG innervation *in vivo*. To remove aggrecan from neonatal dLGN we injected chABC into the dorsal thalamus of *golli-tau-gfp* mice. Numerous studies have used similar approaches to remove CSPGs from brain and spinal cord (Steinmetz et al 2005; Alilain et al. 2011) and have shown that the delivery of chABC can efficiently degrade aggrecan within >1mm of the injection site. For our studies we injected chABC medial to dLGN, ensuring that the injection site did not disrupt dLGN (Figure S2). Our results demonstrate that delivery of chABC into neonatal dLGN increased the extent of CG innervation at P3 compared with uninjected controls or controls injected with penicillinase (PNase), a similarly sized bacterial enzyme with no significant enzymatic activity in brain tissue (Figures 1C and 2G–K).

As an alternative approach, we examined CG innervation in *acan*^{cmd} mutants which lack aggrecan. These mutants die immediately at birth and are underdeveloped compared with littermate controls. In wild-type mice, cortical axons arrive at the ventromedial border of dLGN at birth, therefore despite neonatal lethality in *acan*^{cmd} mutants, we were able to assess whether cortical axons could immediately grow into dLGN at P0 in the absence of aggrecan. Cortical axons were labeled with tau-GFP by crossing *acan*^{cmd} mutants with *golli-tau-gfp* reporter mice. In the absence of aggrecan we observed cortical axons invading dLGN in every P0 *acan*^{cmd} mutant analyzed (n=3)(Figure 2L, M). In contrast, we failed to detect any cortical axons in dLGN of littermate controls at PO (n=3) or in any of our other control mice until after P2 (for example see Figure 1B, E). Two additional features of cortical axons in *acan*^{cmd} mutants warrant mention. First, cortical axons in PO *acan*^{cmd} mutants failed to accumulate adjacent to dLGN. Second, the axons prematurely entering P0 mutant dLGN appeared to be pioneers at the leading-edge of corticothalamic projections. Taken together, these results support that aggrecan is necessary for preventing premature entry of dLGN by cortical axons.

Aggrecanases are upregulated in postnatal dLGN

Surprisingly, despite dramatic changes in aggrecan-IR during postnatal dLGN development, we failed to detect significant differences in expression levels of *acan*, the gene encoding aggrecan (1.3 fold increase from P3 to P8 in dLGN by microarray; p=0.37 by t-test). We therefore suspected that postnatal decreases in aggrecan distribution resulted from its cleavage by proteases. This hypothesis was supported by our discovery that several ADAMTS ('A Disintegrin and Metalloproteinase with Thrombospondin Motifs') family members were enriched in dLGN (Figure 3A,B)(Table S1). The ADAMTS family of metalloproteinases cleaves a wide range of extracellular proteoglycans (Tang 2001). A subset of this family has a particular affinity for cleaving aggrecan and have termed aggrecanases (Stanton et al. 2011; Tortorella and Malfait 2008). Transcriptional analysis (using microarrays and qPCR) revealed that several of these aggrecanases/ADAMTSs are enriched in perinatal dLGN and their expression increases significantly during the first postnatal weeks of development (Figure 3A–C)(Supplemental Table 1). Thus, increases in aggrecanase/ADAMTS expression coincide with decreases in aggrecan-TR in the developing dLGN. *In situ* hybridizations confirmed these findings and further revealed several other interesting features of aggrecanase/ADAMTS expression (Figure 3D–G). First, the upregulation of some ADAMTS mRNAs (such as ADAMTS15) occurred in a ventromedial to dorsolateral gradient in dLGN (Figure 3D) – a feature that resembled the pattern of aggrecan degradation (Figure 1F,H,I). Second, ADAMTS mRNAs were generated by relay neurons in dLGN (Figure 3F,G).

To test whether aggrecanases/ADAMTSs contribute to the timing of CG innervation we injected active, recombinant ADAMTS4 intrathalamically. ADAMTS4 (also called aggrecanase 1) was chosen over other dLGN-derived ADAMTS members for several reasons. First, unlike most ADAMTS members, recombinant forms of ADAMTS4 are commercially available and are enzymatically active. Second, ADAMTS4 has an aggrecan-degrading activity that is several orders of magnitude higher than other ADAMTS members (Tortorella and Malfait 2008). Third, while each ADAMTS member may be capable of cleaving one of several distinct sites within aggrecan's interglobular domain or chondroitin sulfate domain, ADAMTS4 is capable of cleaving the majority of these sites. These features led us to suspect that exogenous delivery of recombinant ADAMTS4 would most effectively degrade dLGN-derived aggrecan. As described above, intrathalamic injections of ADAMTS4 were performed in neonatal *golli-tau-gfp* mice and the extent of CG innervation was assessed at P3. Our data reveal that recombinant ADAMTS4 increased the extent of CG innervation at P3 compared with uninjected controls or PNase injected controls (Figures 2G,H,K and 3H–J). The delivery of both chABC and ADAMTS4 significantly accelerated CG innervation compared with controls but were not statistically different from each other in their ability to stimulate premature CG innervation (p=0.12 by Tukey-Kramer Test) (Figure 2I,J,K and 3H–J). Taken together these results suggest that relay neuron derived aggrecanases contribute to the developmental degradation of aggrecan in dLGN and in the normal timing of CG innervation.

Retinal inputs regulate the timing of aggrecan degradation

We recently reported that surgical or genetic removal of retinal inputs accelerates the timing of CG innervation (Seabrook et al. 2013). For aggrecan to be responsible for regulating CG innervation we hypothesized that its distribution must be significantly reduced by the removal of retinal inputs in dLGN. To test this we examined aggrecan distribution in *math5*$^{-/-}$ mutants, which lack 95% of retinal ganglion cells (Wang et al. 2001). Retinal axons fail to reach the dLGN in these mutants (Seabrook et al. 2013). To label CG axons in these mice, mutants were crossed to *golli-tau-gfp* reporter mice. At P1 GFP-labeled cortical axons were observed entering dLGN in *math5*$^{-/-}$*; golli-tau-gfp* mutants, and the percent

dLGN innervated by cortical axons in these mutants was significantly greater than in *golli-tau-gfp* controls for much of the first week of postnatal development (Figures 1B,E,F–H and 4A–C). Little aggrecan-IR was detected in *math5*$^{-/-}$*; golli-tau-gfp* mutant dLGN, and the percent dLGN containing detectable aggrecan-IR was significantly lower in mutants than controls (Figure 4A,C). Similar decreases in dLGN aggrecan immunoreactivity were observed in P3 wild-type (WT) mice in which retinal inputs were surgically removed by binocular enucleation (BE) (% dLGN occupied by aggrecan-IR at P3: WT = 31.5% +/− 4.6%; BE = 9.8% +/− 3.4%; *math5*$^{-/-}$ = 6.2% +/− 3.6%. n > 3 mice per group. For WT vs BE p=0.002; for WT vs *math5*$^{-/-}$ p=0.002; for BE vs *math5*$^{-/-}$ p=0.76 by Tukey Kramer Test for Difference Between Means). As we described in controls (for later ages), the first regions of *math5*$^{-/-}$*; golli-tau-gfp* mutant dLGN innervated by CG axons were the first regions with diminished aggrecan-IR (see arrows and arrowheads in Figure 4A,E,F). These results support a role for aggrecan in regulating the timing of CG innervation and demonstrate that retinal inputs play an instructive role in regulating aggrecan distribution in dLGN.

Decreased aggrecan protein levels in *math5*$^{-/-}$*; golli-tau-gfp* mutant dLGN were not the result of down-regulation of *acan* mRNA expression levels in the absence of retinal inputs (0.94 fold change in P3 *math5*$^{-/-}$ dLGN vs control by microarray; p=0.84 by t-test). Based upon the developmental upregulation of aggrecanases/ADAMTSs in control dLGN, we suspected that the expression or activity of these metalloproteinases might be regulated by retinal input. To explore this possibility we compared transcriptional profiles in P3 control and *math5*$^{-/-}$*; golli-tau-gfp* mutant dLGN. Several of the aggrecanase/ADAMTS family members appeared modestly increased in the absence of retinal inputs, suggesting they may be responsible for the significant reduction in aggrecan-IR in these mutants (Figure 4E) (*adamts4* 1.33 fold increase in *math5*$^{-/-}$ dLGN [p=0.06 by t-test]; *adamts9* 1.53 fold increase in *math5*$^{-/-}$ dLGN [p=0.1]; *adamts12* 1.68 fold increase in *math5*$^{-/-}$ dLGN [p=0.002]; *adamts14* 1.55 fold increase in *math5*$^{-/-}$ dLGN [p=0.07]; *adamts15* 1.28 fold increase in *math5*$^{-/-}$ dLGN [p=0.13]; *adamts16* 1.42 fold increase in *math5*$^{-/-}$ dLGN [p=0.07]). Moreover, analysis revealed that mRNA expression of the entire ADAMTS family was 27.1% +/− 12.5% increased in P3 *math5*$^{-/-}$ dLGN (vs control; p=0.002 by t-test), whereas similar changes were not observed for other families of extracellular proteases (eg. ADAM family of metalloproteinases – 1.1% +/− 6.8% increased in in *math5*$^{-/-}$ dLGN; p=0.4 by t-test). It is also notable that besides changes in aggrecanase/ADAMTS expression, we detected few significant changes in ECM, growth factors or transmembrane molecules known to affect axonal targeting in *math5*$^{-/-}$ dLGN (Table S2).

Discussion

Here, we sought to elucidate the molecular underpinnings of the distinct timing of CG innervation. We identified a novel role for aggrecan, a repulsive CSPG enriched in neonatal mouse dLGN, in preventing the premature entry of cortical axons into dLGN. Specifically, aggrecan is enriched in dLGN at birth and its loss during postnatal development coincides spatially and temporally with corticogeniculate innervation (Figure 4H). Likewise the expression of endogenous aggrecan-degrading enzymes (i.e. ADAMTSs) corresponds spatially and temporally with diminished aggrecan distribution and cortical innervation of dLGN (Figure 4H). *In vitro* and *in vivo* manipulations support our hypothesis that aggrecan controls the timing of corticogeniculate innervation since aggrecan repels neurites from layer VI cortical neurons and premature removal of aggrecan accelerates CG innervation.

It warrants mention that the dramatic enrichment of aggrecan in neonatal dLGN is somewhat surprising, since this region is a major target of retinal axons and retinal axons are potently repelled by aggrecan *in vitro* (Snow and Letourneau 1992). Here, we found that retinal

ganglion cells express a cohort of CSPG-binding PTPRs (Figure S1) and previous studies show neonatal expression of NgRs by retinal axons (Xiaolei et al. 2009; Wang et al. 2008). Therefore, how retinal axons overcome the inhibitory nature of aggrecan within the neonatal dLGN remains unclear. One possibility is that retinal axons express a cohort of integrin receptors that permit them to grow into aggrecan-rich brain regions, such as integrins α3β1 and α6β1 (Condic et al. 1999; Tan et al. 2011). Indeed, immunostaining revealed that retinal ganglion cells but not cortical neurons express α3 integrin (Figure S3)(Figure 4H). An additional and alternative possibility is that increased expression of neurotrophins in dLGN may permit retinal targeting in an aggrecan-rich environment, as has been shown for other axon types (Zhou et al 2006; Massay et al. 2007). RGCs express neurotrophin receptors and our previous studies revealed that neurotrophin 3 and brain-derived neurotrophic factor are both significantly enriched in perinatal dLGN (Zanellato et al. 1993; Su et al. 2011).

In addition to identifying a novel role for aggrecan in controlling the timing of CG innervation, we demonstrate that the developmental regulation of aggrecan protein is influenced by RG innervation. Thus retinal inputs play an instructive role in the timing of CG innervation by regulating aggrecan degradation. It remains unclear exactly how retinal axons incluence aggrecan distribution in dLGN. However based on our results we propose that retinal inputs initially prevent the expression of endogenous aggrecanases by dLGN relay neurons (Figure 4H). As retinal inputs release this “break” on aggrecanase/ADAMTS expression, relay neurons begin to express and release these enzymes which degrade aggrecan and permit cortical axon entry into dLGN. Support for this hypothesis comes from our results showing reduced aggrecan levels in the absence of retinal axons and a modest increase in ADAMTS mRNA expression in the absence of retinal inputs. We suspect a modest upregulation of several aggrecanases may be sufficient to cause dramatic changes in aggrecan distribution since all are capable of degrading aggrecan. Several alternative possibilities for how retinal inputs govern aggrecan distribution also exist. For example, retinal innervation may alter the activity of aggrecanases/ADAMTSs. Like other metalloproteinases, aggrecanase/ADAMTS activity is inhibited by tissue inhibitors of metalloproteinases (TIMPs) and is activated by other enzymes, such as matrix metalloproteinase 17 (MMP17)(Murphy 2011; Gao et al. 2004). Aggrecanase-activating and inhibiting factors are generated by both retinal ganglion cells and dLGN relay neurons (Figure 3)(Kay et al. 2011), therefore retinal axons may alter aggrecanase/ADAMTS activity either by directly secreting these factors or by inducing relay neurons to secrete them. Alternatively, retinal inputs may also affect the release of aggrecan into the extracellular environment of dLGN. These possibilities are not mutually excusive and may work in concert to regulate aggrecan distribution in the postnatal dLGN.

Finally, cortical axons are not the only non-retinal inputs to innervate dLGN relay neurons. In addition to those from cortex, non-retinal inputs to dLGN arise from superior colliculus, pretectum, brainstem, the thalamic reticular nucleus and local interneurons and account for ~90% of all synaptic inputs onto thalamic relay neurons (Sherman and Guillery 2002; Bickford et al. 2010). The formation of these other non-retinal inputs onto dLGN relay neurons are similarly delayed compared with retinogeniculate circuit formation (Bickford et al. 2010; Singh et al. 2012). It remains unclear whether dLGN-derived aggrecan plays a similar role in delaying the formation of these other non-retinal inputs in dLGN.

EXPERIMENTAL PROCEDURES

Animals

Wild-type mice were purchased from Charles River (Wilmington, MA) or Harlan (Indianapolis, IN). Aggrecan deficient mice (*acan*^{cmd}) were purchased from The Jackson Laboratory (Bar Harbor, ME). The generation of *math5*$^{-/-}$ and *golli-tau-gfp* mice were

described previously (Wang et al., 2001; Jacobs et al., 2007). Genotyping information can be found in Supplemental Experimental Procedures. Binocular enucleations were performed at birth as described previously (Seabrook et al. 2013). All analyses conformed to National Institutes of Health guidelines and protocols approved by the Virginia Polytechnic Institute and State University and Virginia Commonwealth University Institutional Animal Care and Use Committees.

RNA analysis

RNA isolation, reverse transcription, PCR, and real-time quantitative PCR were performed as previously described (Su et al. 2010). Primer sequences can be found in Supplemental Experimental Procedures. Agilent Microarrays were performed by Genus Biosystems (Northbrook, IL) as described previously (Su et al. 2011).

Immunohistochemistry (IHC)

Fluorescent IHC was performed on 16 μm cryosectioned paraformaldehyde-fixed brain tissue or cultured neurons as described previously (Su et al. 2011). Images were acquired on a Zeiss AxioImager A1 fluorescent microscope or a Zeiss 710 confocal microscope. When comparing different ages, treatments, or genotypes, images were acquired with identical parameters. A minimum of three animals (per genotype, treatment or age) were compared in all experiments. Spatial coverage of dLGN by aggrecan and GFP-labeled layer VI fibers was determined using threshold analysis as described previously (Seabrook et al. 2013). A list of the antibodies and additional details can be found in Supplemental Experimental Procedures.

In situ Hybridization (ISH)

Riboprobe generation and *in situ* hybridization were performed as described previously (Su et al. 2010). Anti-sense riboprobes were generated against *syt1*, *adamts4* and *adamts15* (Image Clone ID *syt1*: 5363062; *adamts4*: 5345809; *adamts15:* 30619053; Open Biosystems, Huntsville, AL) and were hydrolyzed to 500 nt.

Intrathalamic Injections

P0-P1 *golli-tau-gfp* mice were anesthetized and injected through the skull using a glass pipette and Picospritzer with either 0.05 U/μl chABC (Sigma), 0.05 U/μl penicillinase (Sigma) or 10 μg/mL rhADAMTS4 (R&D systems). Two days post injection, mice were euthanized, perfused, and IHC was performed. Additional details can be found in Supplemental Experimental Procedures.

In vitro cultures

Cerebral cortices were dissected from E15–E18 *golli-tau-gfp* embryos, dissociated into single cell suspensions and were cultured for 3–4 days in serum-free medium (Neurobasal medium with 0.5 mM L-Glutamine, 25 uM L-Glutamate, 10 ug/ml Gentamicin with B27 supplement). Chamber slides were “spotted” with various extracellular substrates before seeding neurons. Briefly, various concentrations (1 μg/ml, 5 μg/ml and 10 μg/ml) of aggrecan (Sigma), chABC or recombinant human ADAMTS4 (rhADAMTS4, R&D Systems) were mixed with BSA conjugated to Alexa-Fluor 594 (Invitrogen) (2 μg/ml) and 2μl spots were placed onto the slide surface in separate chambers and allowed to incubate in a humidified chamber at 37 °C for two hours. A minimum of four experiments (each with at least 3 replicates) was compared in all *in vitro* experiments. Additional details can be found in Supplemental Experimental Procedures.

Supplementary Material

Refer to Web version on PubMed Central for supplementary material.

Acknowledgments

This project was supported by the National Institutes of Health (Grant #EY012716 to W.G. and Grant #EY021222 to M.A.F.). *Golli-tau-gfp*$^{+/+}$ mice and *math5*$^{-/-}$ mice were generously provided by A.T. Campagnoni and S.W. Wang, respectively.

References

Alilain WJ, Horn KP, Hu H, Dick TE, Silver J. Functional regeneration of respiratory pathways after spinal cord injury. Nature. 2011; 475:196–200. [PubMed: 21753849]

Bickford ME, Slusarczyk A, Dilger EK, Krahe TE, Kucuk C, Guido W. Synaptic development of the mouse dorsal lateral geniculate nucleus. J Comp Neurol. 2010; 518:622–635. [PubMed: 20034053]

Condic ML, Snow DM, Letourneau PC. Embryonic neurons adapt to the inhibitory proteoglycan aggrecan by increasing integrin expression. J Neurosci. 1999; 19:10036–10043. [PubMed: 10559411]

Dickendesher TL, Baldwin KT, Mironova YA, Koriyama Y, Raiker SJ, Askew KL, Wood A, Geoffrey CG, Zheng B, Liepmann CD, et al. NgR1 and NgR3 are receptors for chondroitin sulfate proteoglycans. Nat Neurosci. 2012; 15:703–712. [PubMed: 22406547]

Fisher D, Xing B, Dill J, Li H, Hoang HH, Zhao Z, Yang XL, Bachoo R, Cannon S, Longo FM, et al. Leukocyte common antigen-related phosphatase is a functional receptor for chondroitin sulfate proteoglycan axon growth inhibitors. J Neurosci. 2011; 31:14051–14066. [PubMed: 21976490]

Fox MA, Guido W. Shedding light on class-specific wiring: development of intrinsically photosensitive retinal ganglion cell circuitry. Mol Neurobiol. 2011; 44:321–329. [PubMed: 21861091]

Gao G, Plaas A, Thompson VP, Jin S, Zuo F, Sandy JD. ADAMTS4 (aggrecanase-1) activation on the cell surface involves C-terminal cleavage by glycosylphosphatidyl inositol-anchored membrane type 4-matrix metalloproteinase and binding of the activated proteinase to chondroitin sulfate and heparan sulfate on syndecan-1. J Biol Chem. 2004; 279:10042–10051. [PubMed: 14701864]

Grant E, Hoerder-Suabedissen A, Molnar Z. Development of the corticothalamic projections. Front Neurosci. 2012; 6:53. [PubMed: 22586359]

Huberman AD, Feller MB, Chapman B. Mechanisms underlying development of visual maps and receptive fields. Annu Rev Neurosci. 2008; 31:479–509. [PubMed: 18558864]

Jacobs EC, Campagnoni C, Kampf K, Reyes SD, Kalra V, Handley V, Xie YY, Hong-Hu Y, Spreur V, Fisher RS, Campagnoni AT. Visualization of corticofugal projections during early cortical development in a tau-GFP-transgenic mouse. Eur J Neurosci. 2007; 25:17–30. [PubMed: 17241263]

Kay JN, De la Huerta I, Kim IJ, Zhang Y, Yamagata M, Chu MW, Meister M, Sanes JR. Retinal ganglion cells with distinct directional preferences differ in molecular identity, structure, and central projections. JNeurosci. 2011; 31:7753–7762. [PubMed: 21613488]

Kwok JC, Afshari F, Garcia-Alias G, Fawcett JW. Proteoglycans in the central nervous system: plasticity, regeneration and their stimulation with chondroitinase ABC. Restor Neurol Neurosci. 2008; 26:131–145. [PubMed: 18820407]

Murphy G. Tissue inhibitors of metalloproteinases. Genome Biol. 2011; 12:233. [PubMed: 22078297]

Sanes JR, Zipursky SL. Design principles of insect and vertebrate visual systems. Neuron. 2010; 66:15–36. [PubMed: 20399726]

Seabrook TA, El-Danaf RN, Krahe TE, Fox MA, Guido W. Retinal input regulates the timing of corticogeniculate innervation. J Neurosci. 2013; 33:10085–10097. [PubMed: 23761904]

Shatz CJ, Rakic P. The genesis of efferent connections from the visual cortex of the fetal rhesus monkey. J Comp Neurol. 1981; 196:287–307. [PubMed: 7217358]

Shen Y, Tenney AP, Busch SA, Horn KP, Cuascut FX, Liu K, He Z, Silver J, Flanagan JG. PTPsigma is a receptor for chondroitin sulfate proteoglycan, an inhibitor of neural regeneration. Science. 2009; 326:592–596. [PubMed: 19833921]

Sherman SM, Guillery RW. The role of the thalamus in the flow of information to the cortex. Philos Trans R Soc Lond B Biol Sci. 2002; 357:1695–1708. [PubMed: 12626004]

Singh R, Su J, Brooks J, Terauchi A, Umemori H, Fox MA. Fibroblast growth factor 22 contributes to the development of retinal nerve terminals in the dorsal lateral geniculate nucleus. Front Mol Neurosci. 2012; 4:61. [PubMed: 22363257]

Snow DM, Letourneau PC. Neurite outgrowth on a step gradient of chondroitin sulfate proteoglycan (CS-PG). J Neurobiol. 1992; 23:322–336. [PubMed: 1624935]

Stanton H, Melrose J, Little CB, Fosang AJ. Proteoglycan degradation by the ADAMTS family of proteinases. Biochim Biophys Acta. 2011; 1812:1616–1629. [PubMed: 21914474]

Steinmetz MP, Horn KP, Tom VJ, Miller JH, Busch SA, Nair D, Silver DJ, Silver J. Chronic enhancement of the intrinsic growth capacity of sensory neurons combined with the degradation of inhibitory proteoglycans allows functional regeneration of sensory axons through the dorsal root entry zone in the mammalian spinal cord. J Neurosci. 2005; 25:8066–8076. [PubMed: 16135764]

Su J, Gorse K, Ramirez F, Fox MA. Collagen XIX is expressed by interneurons and contributes to the formation of hippocampal synapses. J Comp Neurol. 2010; 518:229–253. [PubMed: 19937713]

Su J, Haner CV, Imbery TE, Brooks JM, Morhardt DR, Gorse K, Guido W, Fox MA. Reelin is required for class-specific retinogeniculate targeting. J Neurosci. 2011; 31:575–586. [PubMed: 21228166]

Tan CL, Kwok JC, Patani R, Ffrench-Constant C, Chandran S, Fawcett JW. Integrin activation promotes axon growth on inhibitory chondroitin sulfate proteoglycans by enhancing integrin signaling. J Neurosci. 2011; 31:6289–6295. [PubMed: 21525268]

Tang BL. ADAMTS: a novel family of extracellular matrix proteases. Int J Biochem Cell Biol. 2001; 33:33–44. [PubMed: 11167130]

Tortorella MD, Malfait AM. Will the real aggrecanase(s) step up: evaluating the criteria that define aggrecanase activity in osteoarthritis. Curr Pharm Biotechnol. 2008; 9:16–23. [PubMed: 18289053]

Wang J, Chan CK, Taylor JS, Chan SO. Localization of Nogo and its receptor in the optic pathway of mouse embryos. J Neurosci Res. 2008; 86:1721–1733. [PubMed: 18214994]

Wang SW, Kim BS, Ding K, Wang H, Sun D, Johnson RL, Klein WH, Gan L. Requirement for math5 in the development of retinal ganglion cells. Genes Dev. 2001; 15:24–29. [PubMed: 11156601]

Watanabe H, Kimata K, Line S, Strong D, Gao LY, Kozak CA, Yamada Y. Mouse cartilage matrix deficiency (cmd) caused by a 7 bp deletion in the aggrecan gene. Nat Genet. 1994; 7:154–157. [PubMed: 7920633]

Xiaolei Y, Rongdi Y, Shuxing J, Jian Y. The expression patterns of Nogo-A and NgR in the neonatal rat visual nervous system. Neurochem Res. 2009; 34:1204–1208. [PubMed: 19125329]

Zanellato A, Comelli MC, Dal Toso R, Carmignoto G. Developing rat retinal ganglion cells express the functional NGF receptor p140trkA. Dev Biol. 1993; 159:105–113. [PubMed: 8365554]

Zhou FQ, Walzer M, Wu YH, Zhou J, Dedhar S, Snider WD. Neurotrophins support regenerative axon assembly over CSPGs by an ECM-integrin-independent mechanism. J Cell Sci. 2006; 119:2787–2796. [PubMed: 16772333]

HIGHLIGHTS

- Aggrecan, a repulsive CSPG, is enriched in neonatal dLGN
- Layer VI cortical axons are repelled by aggrecan
- Premature removal of aggrecan accelerates corticogeniculate innervation
- Retinal inputs play an instructive role in the timing of aggrecan loss from dLGN

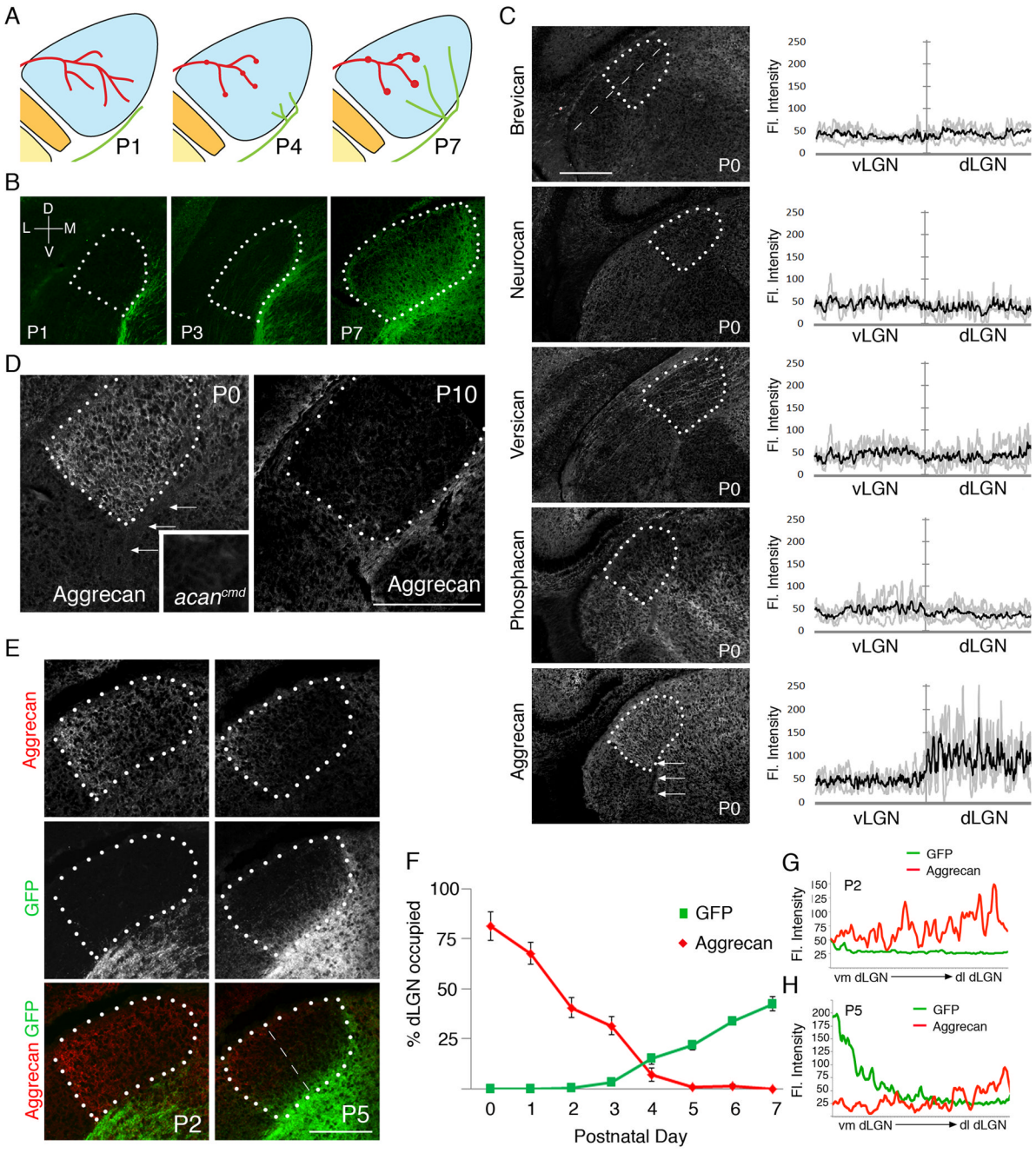

Figure 1.

Developmental regulation of aggrecan in postnatal dLGN. **A.** Schematic depiction of the timing of retino- and corticogeniculate innervation. Retinal axons are shown in red; cortical axons are shown in green. Synapses are illustrated by red or green dots. **B.** Development of corticogeniculate projections in *golli-tau-gfp* transgenic mice. Projections from layer VI cortical neurons are labeled with tau-GFP in these mice. For all panels dLGN are encircled by white dots. D – dorsal; V – ventral; M- medial; L – lateral. **C.** Immunostaining revealed aggrecan but not other CSPGs was enriched in P0 mouse dLGN. Arrows depict eml. Fluorescent intensities were measured with a line scan along the ventrolateral to dorsomedial axis of LGN (see dashed line). Fluorescent intensities in vLGN and dLGN are

plotted. Grey lines represent IR in individual animals (n=4) and black line represents mean of all experiments. **D.** Developmental regulation of aggrecan distribution during the first 2 weeks of postnatal dLGN development. Inset shows a lack of aggrecan-IR in dLGN of an aggrecan-deficient mutant (*acan*^{cmd}). **E.** Aggrecan-IR and GFP-IR in dLGN of P2 and P5 *golli-tau-gfp* transgenic mice. Note the first regions occupied by cortical axons lack aggrecan-IR. **F.** The percentage of dLGN occupied by aggrecan-IR was measured in *golli-tau-gfp* transgenic mice for the first 8 days of postnatal development. The percentage of cortical innervation in these mice was also quantified. Data are shown +/− SEM. **G,H.** Fluorescent intensities in **E** were measured with a line scan along the ventromedial (vm) to dorsolateral (dl) axis of LGN (see dashed line in **E**). Mean fluorescent intensities from 4 P2 (**G**) and P5 (**H**) *golli-tau-gfp* mice are plotted for GFP- and aggrecan-IR. Scale bars = 250 μm.

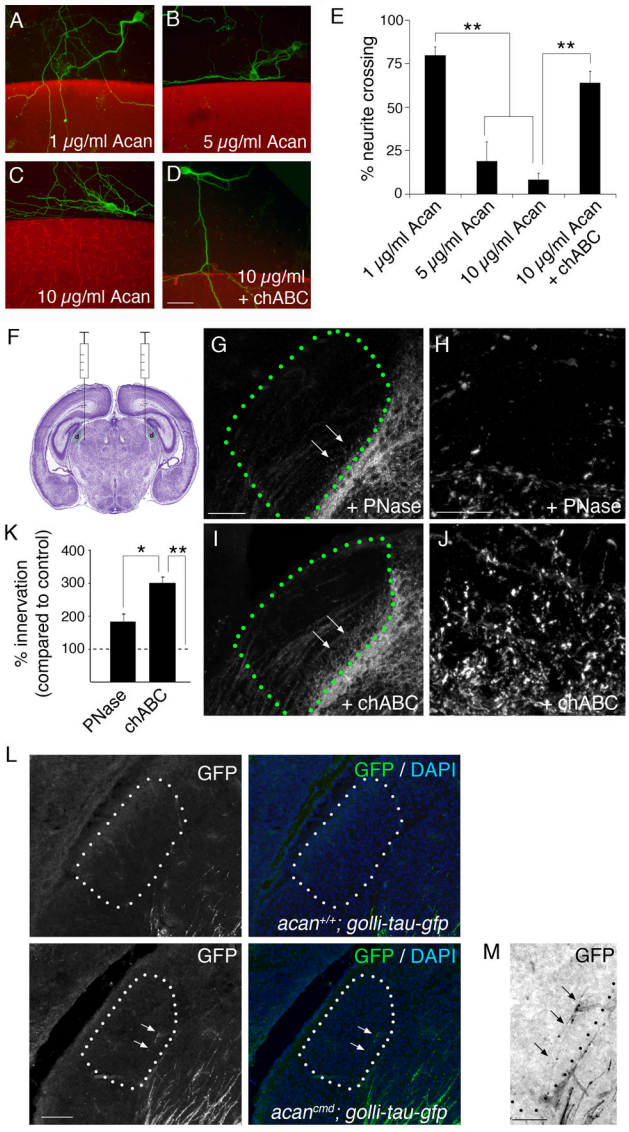

Figure 2.

Aggrecan inhibits cortical axon outgrowth. **A–D.** Modified stripe assays demonstrate that high concentrations of aggrecan (Acan)(**B,C**) inhibit neurite outgrowth from layer VI neurons isolated from *golli-tau-gfp* transgenic mice. Pretreatment of 10 μg/ml aggrecan with chABC alleviated its growth-inhibitory properties (**D**). Aggrecan-containing substratum depicted in red; tau-GFP-expressing neurons shown in green. **E.** Quantification of the percentage of neurites capable of crossing into aggrecan-containing substrata shown in **A–D.** Data are shown +/−SEM: n>4 experiments in triplicate. ** Differ by p<0.01 by Tukey-Kramer Test. **F.** Schematic depiction of the site of our bilateral intrathalamic injections. Image of the cresyl violet stained brain modified from Allen Institute of Brain Science. **G–J.** GFP-labeled axon invasion of P3 dLGN following intrathalamic injection of PNase (**G,H**) or chABC (**I,J**) in P0 *golli-tau-gfp* transgenic mice. Delivery of chABC accelerated the rate of CG innervation. **H,J.** High magnification images of GFP-IR in areas highlighted by arrows in **G** and **I** respectively. **K.** Quantification of the percent dLGN innervated by GFP-containing cortical axons following injection of PNase or chABC. Data are normalized to

data obtained from uninjected *golli-tau-gfp* littermates and are shown +/− SEM: n>4. ** chABC treatment differs from uninjected controls by p<0.0005 by Tukey-Kramer Test. *chABC treatment differs from PNase treatment by p<0.02. PNase treatment and uninjected controls were not statistically different. **L,M.** Cortical axons invade dLGN at P0 in *acan*^{cmd}*; golli-tau-gfp* mutants (see arrows). dLGN encircled by dots. Nuclei were labeled with DAPI to determine dLGN boundaries. **H.** High-magnification of tau-GFP labeled cortical axons in P0 dLGN shown in **L.** Signal has been inverted to enhance detection of thin caliber cortical axons. dLGN encircled by dots. Scale bar in **D** = 50 μm for **A–D,** in **G** = 150 μm for **G,I,** in **H** = 20 μm for **H,J,** in **L** = 100 μm, and in **M** = 50μm.

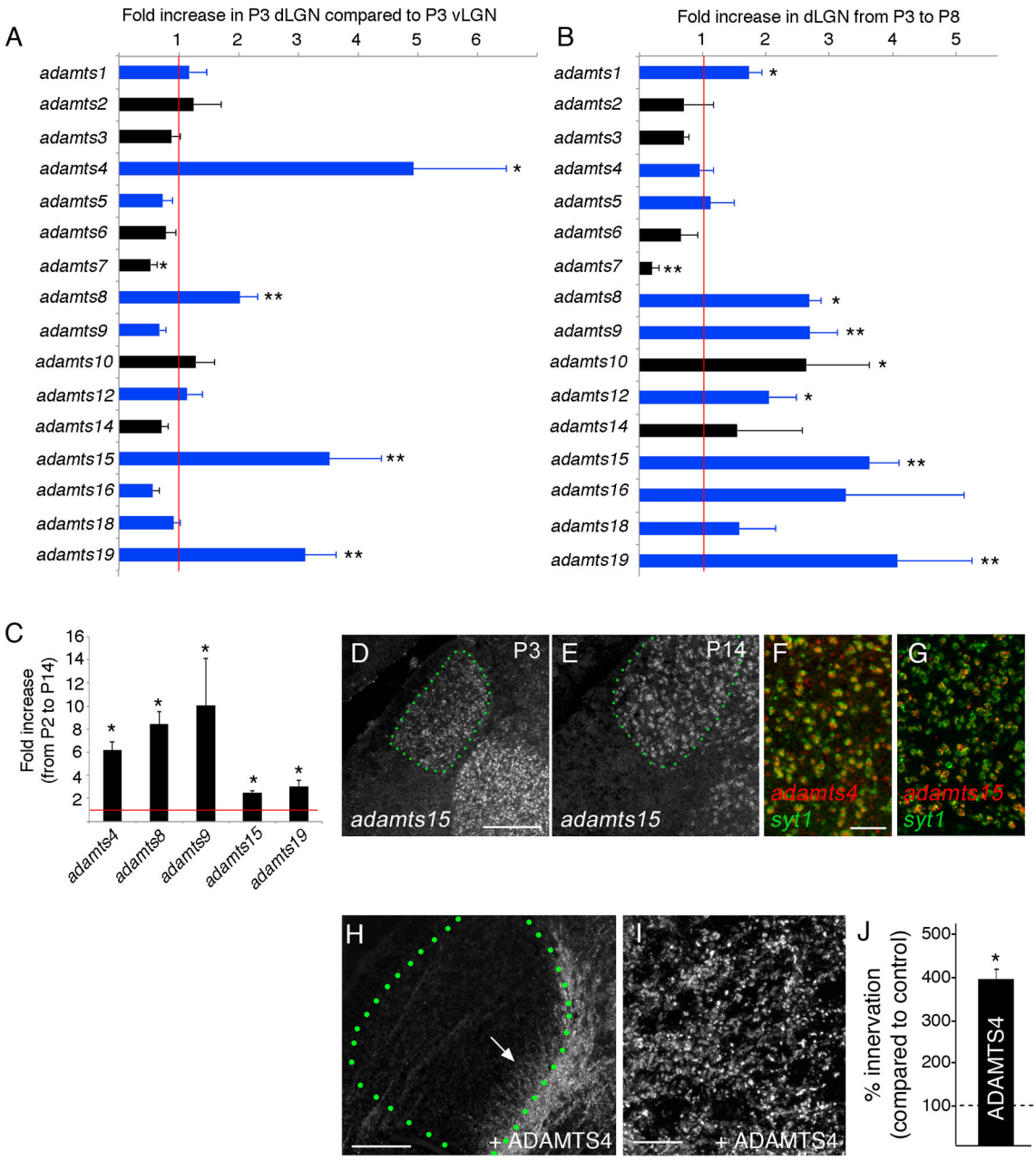

Figure 3.

Aggrecanases are upregulated in postnatal dLGN. **A.** Microarray revealed that several members of the ADAMTS family of metalloproteinases are enriched in P3 dLGN compared to adjacent thalamic regions (vLGN). Expression of ADAMTS genes with known aggrecan-degrading activity are colored in blue. Red line represents no change in gene expression. Data are shown +/− SEM: n=3. * differs by p<0.05 by T=test; ** differs by p<0.01. **B.** Microarray demonstrates upregulation of several aggrecan-degrading ADAMTS members in dLGN from P3 to P8. Expression of ADAMTS genes with known aggrecan-degrading activity are colored in blue. Data are shown +/− SEM: n=3. * differs by p<0.05; ** differs by p<0.01. **C.** qPCR confirmed the upregulation of aggrecanases in dLGN from P2 to P14. Data are shown +/− SEM: n=3. * differs by p<0.001. **D,E.** *In situ* hybridization (ISH) of

adamtsl5 mRNA in P3 and P14 LGN. dLGN encircled by green dots. **F,G.** Double-ISH revealed that *adamts4* (**F**) and *adamtsl5* (**G**) mRNAs are expressed by *syt1*-expressing neurons in dLGN. **H.** GFP-labeled axon invasion of P3 dLGN following intrathalamic injection of ADAMTS4. **I.** High magnification image of GFP-IR in area highlighted by arrow in **H. J.** Quantification of the percent dLGN innervated by GFP-containing cortical axons following injection of ADAMTS4. Data are normalized to data obtained from uninjected *golli-tau-gfp* littermates and are shown +/− SEM: n>4. * ADAMTS treatment differs from uninjected controls or PNase treatment by $p<0.0001$ by Tukey-Kramer Test. ADAMTS treatment and chABC treatment were not statistically different. Scale bar in **D** = 200 μm for **D,E,** in **F** = 75 μm for **F,G,** in **H** = 150 μm, and in **I** = 20 μm.

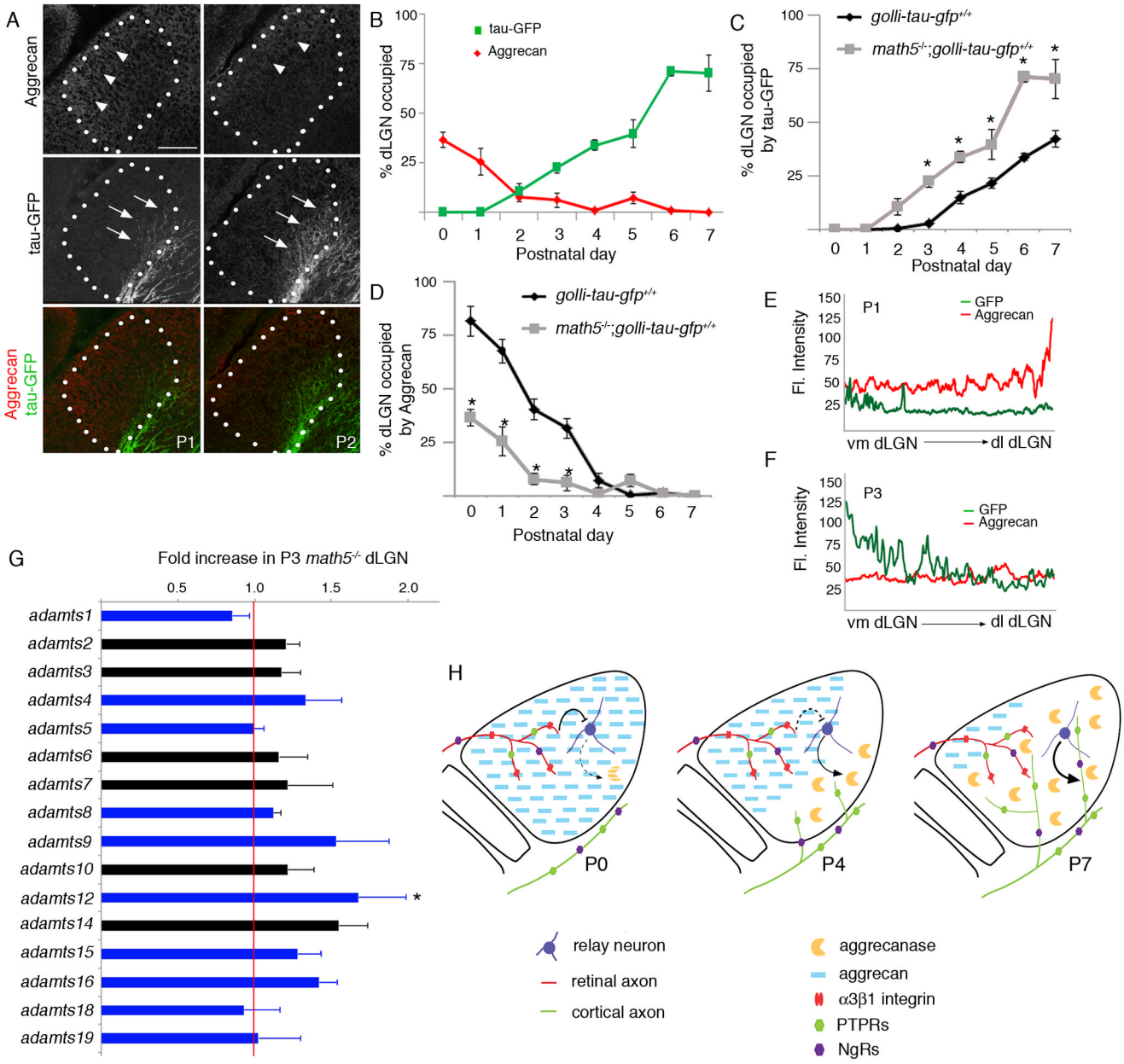

Figure 4.

Retinal inputs influences the degradation of aggrecan in dLGN. **A.** Aggrecan-IR in *math5*$^{-/-}$*; golli-tau-gfp* mutant dLGN which lacks retinal inputs. Arrowheads depict remaining aggrecan-IR in the lateral aspect of dLGN. Arrows highlight GFP-labeled axons prematurely invading dLGN. Note that aggrecan is absent from sites of cortical axon invasion. dLGN are encircled by white dots. **B.** The percentage of dLGN occupied by aggrecan-IR was measured in *math5*$^{-/-}$*; golli-tau-gfp* mutants for the first 8 days of postnatal development. The percentage of dLGN occupied by tau-GFP-expressing cortical axons was also quantified. Dashed line represented the age at which the percent occupied by GFP and aggrecan were equal in controls (see Figure 1G). **C,D.** The percent dLGN occupied by tau-GFP-expressing axons or by aggrecan-IR was compared in *math5*$^{-/-}$*; golli-tau-gfp* mutants and *golli-tau-gfp* controls. Data are shown +/−SEM. * Differ with age-matched

controls by P<0.01 by Tukey-Kramer test. **E,F.** Fluorescent intensities in **A** were measured with a line scan along the ventromedial (vm) to dorsolateral (dl) axis of LGN (see example in Figure 1G,H). Mean fluorescent intensities from 4 P1 and P3 *math5*$^{-/-}$*;golli-tau-gfp* mice are plotted for GFP- and aggrecan-IR. **G.** Microarray analysis revealed some *adamts* mRNAs are modestly upregulated in P3 dLGN in *math5*$^{-/-}$ mutants (compared with wild-type controls). Expression of ADAMTS genes with known aggrecan-degrading activity are colored in blue. Red line represents no change in gene expression. Data are shown +/− SEM: n=3. * differs by p<0.05 by t-test. Scale bar = 100 μm. **H.** Schematic depicting the mechanism by which aggrecan controls the timing of corticogeniculate innervation. See discussion for details.